Simulation of the dynamic behaviour of a geared transmission on hydrodynamic journal bearings

Romain Fargere, Jean-Francois Sigrist, Raphael Bosio, Christian Menard, Philippe Velex

ACOUSTICS 2012

Simulation of the dynamic behaviour of a geared transmission on hydrodynamic journal bearings

R. Fargere, J.-F. Sigrist, R. Bosio, C. Menard and P. Velex

LaMCoS / DCNS Research - Département Dynamique des Structures, DCNS Propulsion, Indret, 44620 La Montagne, France
romain.fargere@insa-lyon.fr

This article deals with the static and dynamic interactions between journal bearings and gears in mechanical transmissions. The proposed approach combines classic lumped parameter and shaft elements, a specific wide-faced spur or helical gear model and external bearing forces. Bearing reactions are determined based on the linearized and non-linear solution to the Reynolds equation for short bearings. The corresponding parametrically excited non-linear state equations are solved by inserting a Newton-Raphson's method and a unilateral normal contact algorithm into a Newmark's time-step integration schema. Finally, the influence of bearing non-linearity, external and internal forcing terms is analyzed on several single stage reduction units with spur and helical gears.

1 Introduction

Although gear vibration and noise do not necessarily impact durability, they are detrimental in terms of perceived quality and should be minimized in certain sensitive applications for which stealthiness is crucial, such as marine propulsion. In these applications, hydrodynamic journal bearings are commonly employed in high speed, high power conditions mostly because of their interesting damping properties. Despite the instability problem in some particular conditions, these properties confer them a better durability and reduced noise compared with rolling element bearings. From a modeling point of view, the classic approach consists in using the dynamic stiffness and damping coefficients determined from a linearized solution to the Reynolds equation in the vicinity of steady state positions. However, journal bearings cannot be considered as purely passive elements since they can generate self-excited vibrations and instabilities. The literature on journal bearings is vast [1-3] and their behavior can be predicted with great accuracy for a number of conditions: misalignments, deformable shafts and bearings, oil injection, thermal effects, non Newtonian lubricant, etc.

On the other hand, the dynamic response of geared transmissions has been extensively analyzed over the last 30 years based on increasingly refined models [4,5] which, for most of them, combine rigid gears, discrete stiffness and damping elements [6,7]. Later, varying mesh stiffness (due to tooth elasticity) and mounting errors or tooth shape modifications (to compensate for elastic deflections under load) are introduced [8]. More recently, gear body deformations are considered using various mechanical models such as shaft [9] or 3-dimensionnal solid finite elements.

Even though both journal bearings and gears have been extensively studied, very few studies deal with the behaviour of fully coupled systems. Most of the models do not consider either bearing [10] and/or gear mesh nonlinearity [11]. This presentation combines the wide faced gear model presented in [9] supported by bearings whose reactions are calculated solving the lubrication equation presented in [3] under the short bearing approximation. Bearing reactions are calculated both with a linear and nonlinear theories as a response to the internal excitation produced by the tooth elasticity. Their evolution is supposed to be directly representative of the acoustical signature of a transmission, even if a more complete study could be led reintroducing these reactions in an acoustic model of the gearbox housing (using boundary elements for instance [12]).

This article presents a mechanical model treating the problem of radiated noise as a vibration problem. A partially linear and a fully nonlinear approach are compared They require a complex solving procedure, based on an accurate static solution and combining (*i*) a Newmark's time-step integration schema, (*ii*) a Newton-Raphson's method and (*iii*) a unilateral normal contact algorithm in order to simultaneously treat the structure problem and the contact problems between the tooth and at each bearing.

The algorithms are applied to a realistic single stage transmission. Simulation results are compared to experimental measurements and the influence of the helix angle is emphasised, justifying the use of helical gears in some applications.

Nomenclature

($\mathbf{s_0}$,$\mathbf{t_0}$,$\mathbf{z_0}$): initial global frame, linked with the center lines

Meshing and coupling

α_t : apparent pressure angle

β_b: base helix angle

C_m, C_r: input, output torque

f_m: mesh frequency (f_m=$Z_1.\Omega_1/2\pi$) ; T_m: mesh period (T_m=1/ f_m)

R_{b1}, R_{b2}: base radius of pinion, of wheel

$\mathcal{R}$: dynamic coefficient $\mathcal{R}$= max(F_{mesh}(t)/$F_{mesh\ 0}$)

Ω_1, Ω_2: rotation speed of pinion shaft, gear shaft

$\mathbf{X_R}$: displacement vector associated with rigid body motion

$\mathbf{X}$: displacement vector associated with elastic displacements

Z_1, Z_2 : number of teeth on pinion, on wheel

Bearings

L : bearing length

C : radial clearance

D : diameter; $R=D/2$

p : pressure field

h : lubricant film height

Ω : rotation speed of considered bearing

μ : dynamic viscosity

Subscripts

b : magnitude related to bearings

M : magnitude related to meshing

S : magnitude related to shafts

C : magnitude related with elastic couplings

0 : corresponding static magnitude.

2 Mechanical model

2.1 Gear, shaft model (examples in annex A)

As represented on figure 1, and neglecting tooth friction, the load is transmitted from the pinion to the gear normally to the tooth surface, i.e. in the line of action direction. For helical gears ($\beta_b \neq 0$, fig. 1), the reaction remains normal to the contact lines whose position, number and total length may vary as long as the meshing process occurs; in the base plane. Both gear bodies and tooth are deformable. At a modeling point of view, the pinion and gear bodies are treated as two shafts in bending, torsion and traction (6 degrees of freedom) and their displacements are approximated by using two-node classic shaft elements (Timoshenko's beam formulation for bending). Tooth

elasticity is modelled using elemental stiffness elements, distributed along the contact lines, such that the total stiffness is proportional to the total length of contact. These stiffness k_{ij} are calculated as the combination of structural deflections [13] (tooth bending and base) and contact compliance [14]. Tooth shape deviations and mounting errors are simulated as initial discrete separations $\delta e(M_i)$ [8].

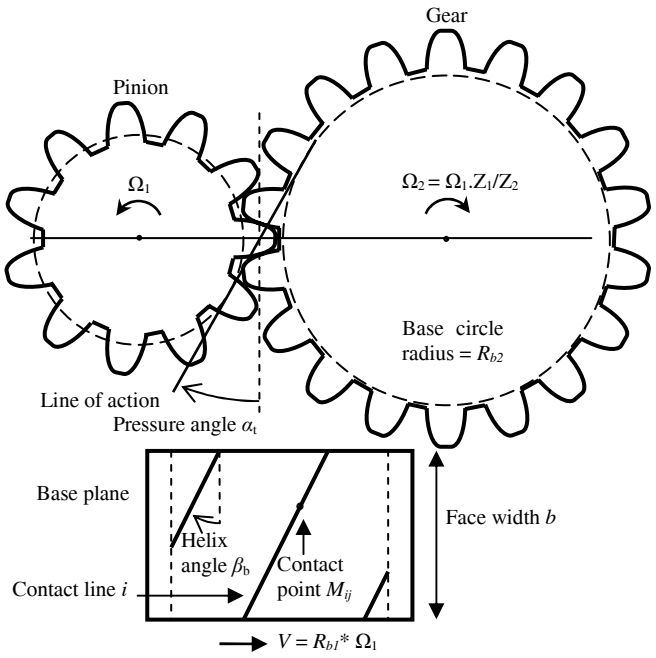

Figure 1: Basic gear geometry and kinematics

The connection element is built by calculating the deflection $\Delta(M_{ij})$ at each point M_{ij}:

$$\Delta\left(M_{ij}\right)=\sum_{m=1}^{2}\left[\left[\mathbf{P_m}\left(M_{ij}\right)\right]\mathbf{U_m}\left(M_{ij}\right)\right]^T\mathbf{q_m}-\delta e\left(M_{ij}\right). \quad (1)$$

where m=1 for the pinion and m=2 for the gear; $\mathbf{U_m}$ is a structure vector; $\mathbf{P_m}$ is the shape function matrix of two-node shaft element m at point M_{ij}; $\mathbf{q_m}$ is the degree-of-freedom vector of shaft element m.

The corresponding local contact force is given by $k_{ij}\Delta(M_{ij})$ from which, the sum of the external forces and moments on pinion and gear can be directly deduced leading to the definition of a gear stiffness matrix $[\mathbf{K_M}(t,\mathbf{q})]$ and a forcing term caused by tooth shape deviations $\mathbf{F_M}(t,\mathbf{q},\delta e(M_{ij}))$, with $\mathbf{q}^T=\{\mathbf{q_1}^T\ \mathbf{q_2}^T\}$.

It is checked that each element is in compression (and that no compressive element is ignored) during the process, using a normal contact algorithm leading to several updates of the stiffness matrix and forcing terms. Further details about the mathematical developments can be found in [8].

2.2 Short bearing model

In the presented work, bearing reactions are considered as external forces acting on the shaft on the corresponding node. Physically, a journal bearing is made of a shaft rotating inside a fixed journal, both parts being separated by a lubricant film, as shown in figure 2. The fluid shearing creates a pressure field (and a load capacity); governed by the Reynolds equation presented in [3].

The Reynolds equation is simplified assuming that $\partial p/\partial z >> \partial p/\partial\theta$ while $L < D$, which makes it analytically solvable.

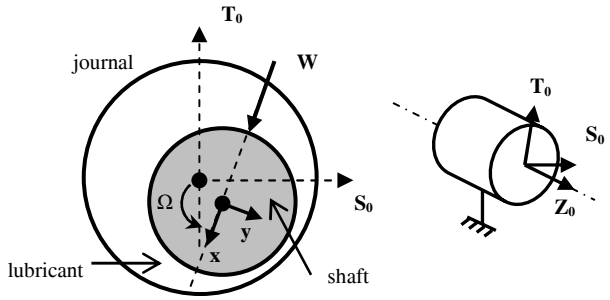

Figure 2: Journal bearing and external load

The bearing reactions in static $\mathbf{F_{b0}}$ and dynamic $\mathbf{F_b}$ cases are calculated integrating the pressure field:

$$\mathbf{F_{b(0)}}=\begin{pmatrix}F_{bx(0)}\\F_{by(0)}\end{pmatrix}_{(\mathbf{x};\mathbf{y})}=\begin{pmatrix}\int_{-L/2}^{L/2}\int_0^{2\pi}p_{(0)}(\theta,z)\cos\theta.R.d\theta.dz\\\int_{-L/2}^{L/2}\int_0^{2\pi}p_{(0)}(\theta,z)\sin\theta.R.d\theta.dz\end{pmatrix}_{(\mathbf{x};\mathbf{y})} \quad (2)$$

The dynamic reaction can be linearized in the vicinity of the static equilibrium position $\mathbf{u_0} = (x_0\ y_0)^T$, so that with $\mathbf{u} = (x\ y)^T$:

$$\mathbf{F_b}(\mathbf{u},\dot{\mathbf{u}})=\mathbf{F_{b\,0}}(\mathbf{u_0})-\left[\mathbf{K_b}(\mathbf{u_0})\right](\mathbf{u}-\mathbf{u_0})-\left[\mathbf{C_b}(\mathbf{u_0})\right](\dot{\mathbf{u}}-\dot{\mathbf{u}}_0) \quad (3)$$

where $[\mathbf{K_b}(\mathbf{u_0})]$ and $[\mathbf{C_b}(\mathbf{u_0})]$ respectively represent the elastic and dissipative effects of the fluid film. Analytical formulations of $\mathbf{F_{b0}}$, $\mathbf{F_b}$, $[\mathbf{K_b}]$ and $[\mathbf{C_b}]$ can be found in [3].

2.3 Coupled systems

Gear dynamics require an accurate reference position for the calculation of the elastic displacements. This reference position corresponds to the rigid body motion of the shafts inside their bearing clearances and results on the equilibrium between rigid shafts and the external forces. This position induces a modified center distance, pressure angle, and shaft misalignments treated as mounting errors.

Related to this reference position, and introducing the displacement vector associated with rigid body motion $\mathbf{X_R}$, the elastic displacement field $\mathbf{X}$ is solution of the equations of motion:

$$\begin{aligned}&\left[\mathbf{M_S}\right]\ddot{\mathbf{X}}+\left[\mathbf{C}\right]\dot{\mathbf{X}}+\left[\mathbf{K_S}+\mathbf{K_M}(t,\mathbf{X})+\mathbf{K_C}\right]\mathbf{X}=\mathbf{F_{ext}}(t)\\&+\sum_{i=1}^{N_b}\mathbf{F_{b\,i}}\left(\mathbf{X},\dot{\mathbf{X}}\right)+\mathbf{F_M}(t,\mathbf{X})-\left[\mathbf{K_C}\right]\mathbf{X_R}\end{aligned} \quad (4)$$

where $[\mathbf{M_Z}]$, $[\mathbf{C_Z}]$ and $[\mathbf{K_Z}]$ are respectively the mass, damping and stiffness matrices related to magnitude $\mathbf{Z}$ referenced in nomenclature, $\mathbf{F_{ext}}$ is the external load vector containing the proper weight of the system, input and output torques and mass imbalance effects.

The dynamic simulation is initiated with the static deformed shape $\mathbf{X_0}$, solution of:

$$\left[\mathbf{K_S}+\overline{\mathbf{K_M}}+\mathbf{K_C}\right]\mathbf{X_0}=\mathbf{F_{ext}}+\sum_{i=1}^{N_b}\mathbf{F_{b0\,i}}(\mathbf{X_0})-\left[\mathbf{K_C}\right]\mathbf{X_R} \quad (5)$$

Linearizing the bearing reaction forces in the vicinity of the position of equilibrium $\mathbf{X_0}$, the equations of motion become:

$$\begin{aligned}&\left[\mathbf{M_S}\right]\ddot{\mathbf{X}}+\left[\mathbf{C}+\mathbf{C_b}\right]\dot{\mathbf{X}}+\left[\mathbf{K_S}+\mathbf{K_M}(t,\mathbf{X})+\mathbf{K_C}+\mathbf{K_b}\right]\mathbf{X}=\\&\mathbf{F_{ext}}(t)+\sum_{i=1}^{N_b}\mathbf{F_{b0\,i}}(\mathbf{X_0})+\mathbf{F_M}(t,\mathbf{X})-\left[\mathbf{K_C}\right]\mathbf{X_R}+\left[\mathbf{K_b}\right]\mathbf{X_0}\end{aligned} \quad (6)$$

3 Simulation results

In this section, the gear sets defined in Table 1-3 and figure 3 are analyzed using both the linear and non-linear theories. The influence of elastic couplings is considered by introducing radial stiffness elements k_r = 5 10^7 *N/m*, with no clearance, at the motor and the brake/propeller node.

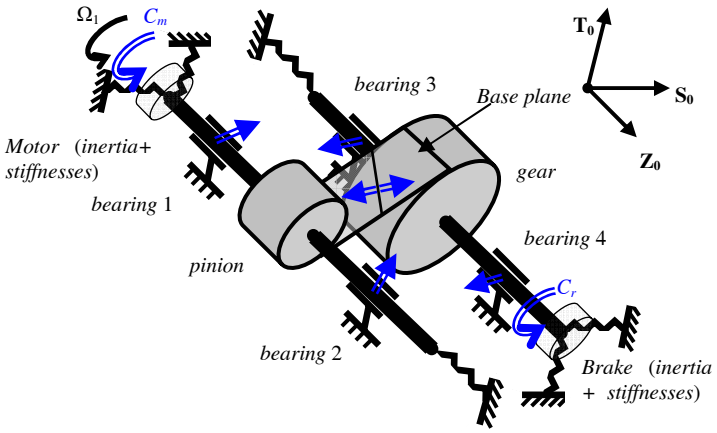

Figure 3: Geared system on journal bearings with initial global frame and some modeling elements.

Table 1: Gear data

	Pinion	Gear
Tooth number	*26*	*157*
Face width (mm)	*50*	*40*
Helix angle (°)	*0 - 10*	
Module (mm)	*4*	
Pressure angle (°)	*20*	

Table 2: Shaft data

	Pinion shaft	Gear shaft
Outer diameter (mm)	*70*	*90*
Inner diameter (mm)	*30*	*30*
Shaft length (mm)	*640*	
Gear Bearing distance (mm)	*320* (pinion and gear are centered)	
Young modulus (MPa)	*210 000*	
Poisson's ratio	*0.3*	
Density (kg/m^3)	*7 800*	
Thrust bearing stiffness (N/m)	*5. 10^5*	

Table 3: Bearing data

	Bearings 1 & 2	Bearings 3 & 4
Diameter(mm)	*70*	*90*
Length (mm)	*50*	*65*
Radial clearance (µm)	*75*	*55*
Lubricant viscosity (Pa.s)	*0.01*	*0.01*

The dynamic behaviour of the geared system is supposed to be represented by the so called "dynamic coefficient", $\mathcal{R}$, defined as the maximum of the ratio between the dynamic and the static force transmitted by the gear pairs. Experimentally [10], this coefficient is estimated using the foot tooth stress at different locations, which allows a comparison with the simulated coefficient, when the pinion speed varies, figure 4. The results present a good agreement, especially for the identification of the critical speeds. The damping coefficients of the model (0.03 in this study) could be calibrated differently so that the amplitude levels fit better with the experimental results.

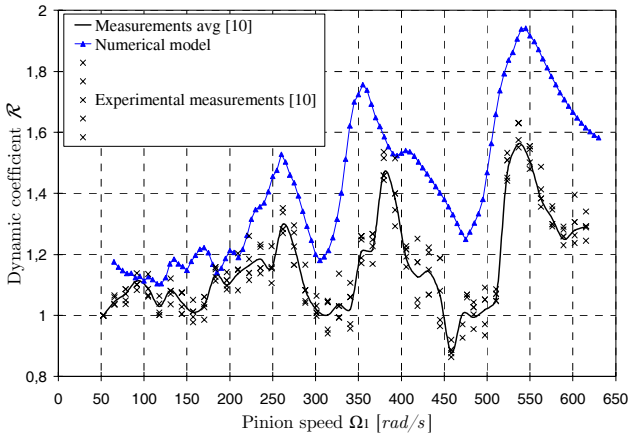

Figure 4: Comparisons of the experimental [10] and numerical dynamic coefficients $\mathcal{R}$ (C_m = 255 *N.m*).

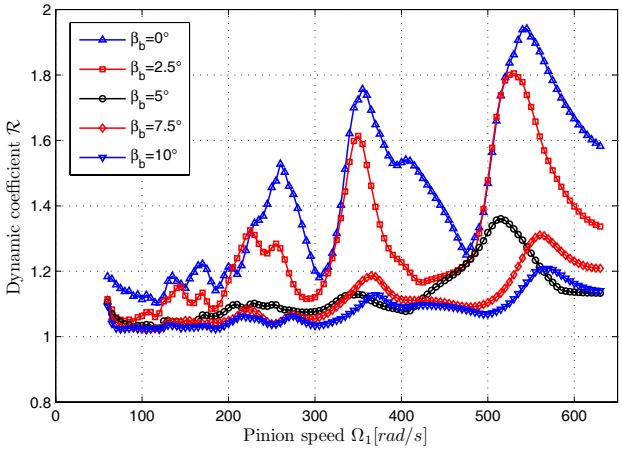

Figure 5: Influence of the helix angle on the dynamic amplification of tooth loading $\mathcal{R}$ (C_m = 255 *N.m*).

Figure 5 shows that increasing the helix angle β_b globally tends to reduce the dynamic coefficient and slightly modifies the critical speeds. The rest of the article presents the study of the reactions of bearings 1 and 2 (pinion shaft), by time or frequency representations, and the study of the RMS of the reactions over the last 5 mesh periods.

The comparison of the RMS of the bearing reactions (figure 6) confirms the results of figure 5, with some additional informations: a significant helix angle tends to reduce the vibration level of the bearings (so as the dynamic coefficient), which is the reason why manufacturers prefer helical gears despite the axial reaction they are responsible for. But the more the helix angle increases, the more the system becomes asymmetric and the more the bearings have particular behaviours. For spur gears (β_b = 0), bearings 1 and 2, present very similar responses but as long as β_b increases, each bearing tends to have its own behaviour and critical speeds, which make a fully coupled model necessary.

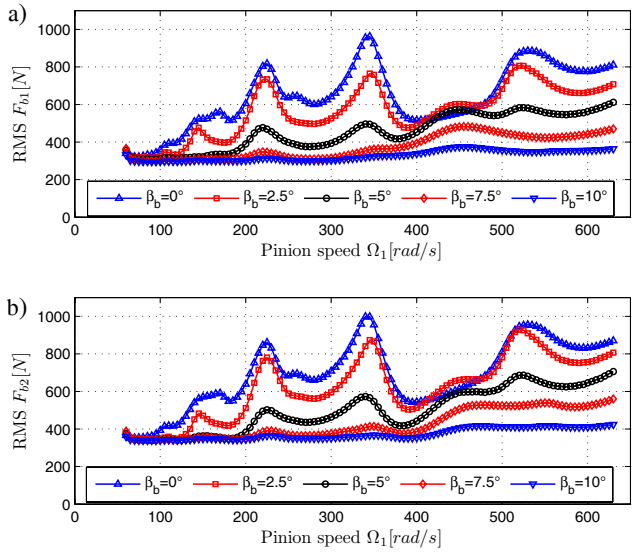

Figure 6: Influence of the helix angle on the RMS bearing reactions (C_m = 255 *N.m*). a) bearing 1 ; b) bearing 2

Figures 5 and 6 show that the system has very different behaviours at different regimes, which is partially due to the particular behaviour of journal bearings. Even though a linear theory is a rather good approximation, figure 7 shows several informations:

- the bearings are excited at multiples of the mesh frequency (only five harmonics represented, the two firsts are prevailing) which are transmitted to the gearbox housing;
- in the presence of imbalance (0.2 *mm* on the center of mass of pinion and gear), nonlinear calculations are necessary as the response of bearing 1 significantly varies between the linear and nonlinear models.

It is worth noting that on the time representation figure 7.b), an amplitude modulation phenomena is present, which is smaller with the linear formulation 7.a). As a consequence, some lateral bands appear on the FFT representation of F_{b1} 7.b) at frequencies $f = n.f_m \; \emptyset \; k.\Omega_1/2\pi$, $(k;n) \in \text{IN}^2$, whereas they are almost missing on 7.a). Based upon the amplitude of the lateral bands of each harmonic, the modulation index m_i of the *i-th* harmonic is $m_1 \approx 0.07$; $m_2 \approx 0.15$ (nonsymmetrical) in the linear case and $m_1 \approx 0.2$; $m_2 \approx 0.15$ with the nonlinear model, which is non-negligible for a very sharp study. Moreover, the levels of each harmonic are significantly different with both theories. The bearings response to imbalance appears at the first band on FFT representations ($f = \Omega_1/2\pi$) and the nonlinear formulation makes two smaller bands visible at multiples of the rotational frequency ($f = (1+k).\Omega_1/2\pi$, k = 1,2).

For helical gears, bearing 1 (figure 7.c) presents a comparable low frequency behaviour (bands at $f = (1+k).\Omega_1/2\pi$, k = 0,1,2) but very small dynamic perturbations (with some amplitude modulation phenomena). The other bearings present a very different behaviour and the system becomes totally asymmetric which modifies tooth loading and make an accurate model necessary. In applications where stealthiness is crucial, double-helical gears are sometimes prefered because they don't generate axial thrust, keep the system symmetrical and generate small vibrations; in spite of their slightly lower efficiency.

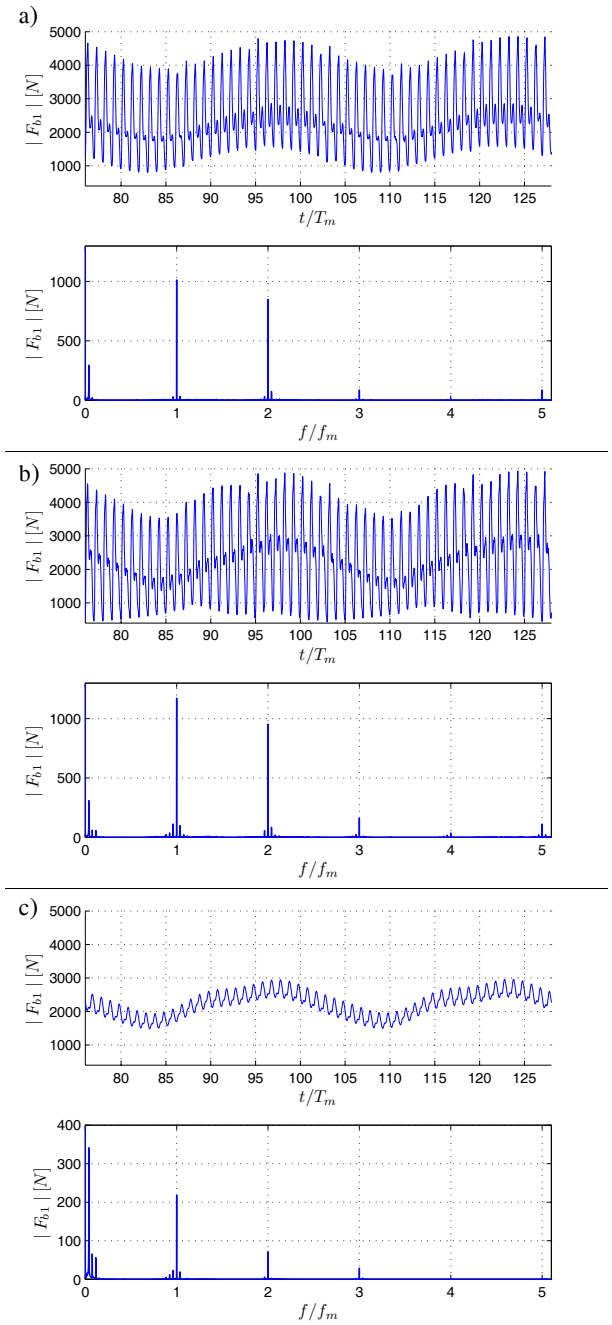

Figure 7: Influence of the bearing model and helix angle on the reaction of bearing 1: time representations over two pinion revolutions and FFT (Ω_1 = 525 *rad/s* ; C_m = 255 *N.m*). a) β_b = 0° linear theory ; b) β_b = 0° nonlinear theory ; c) β_b = 10° nonlinear theory

4 Conclusion

A fully coupled mechanical model is presented. It is aimed at simulating the dynamic behaviour of a single stage geared transmission similar to those used for marine propulsion. The response on the structure is analysed through the bearing reactions and at a mechanical point of view, with several criterion related with the tooth contact. The results of the numerical simulations present a good accordance with the experimental measurements. Simulations reveal that some modulation phenomena clearly appear which are stronger with the non linear model. The interest of helical gears is emphasized through a parametric study, which reinforces the choice of using

helical gears for applications where stealthiness is essential. The main disadvantage of this solution being the axial thrust, it is usually evaded using double helical gears, which compensate this axial thrust.

Finally, a logical continuation to this work concerns the refinement of the prediction of the radiated noise from the transmission: this model could be coupled with an acoustical model of the gearbox housing.

Annex A: Involute gear types

Spur gears

Figure A1: Example of spur gear

+ Simple geometry / manufacturing, good efficiency
+ Simple load transfer
+ No axial thrust
- Important mesh stiffness variations, and vibration level

Helical gears

Figure A2: Example of helical gear

+ Simple geometry (but more complex modelling)
+ Low mesh stiffness variations, and vibration level
- More complex load transfer
- Axial thrust

Double helical gears

Figure A3: Example of double-helical gear set

+ Low mesh stiffness variations, and vibration level
+ Simple load transfer
+ No axial thrust
- More complex manufacturing
- More power losses (important for high power applications)

References

[1] Cameron, A., "The Principles of lubrication", Longmans (1966)

[2] Pinkus, O. and Sternlight B., "Theory of Hydrodynamic Lubrication", Mc Graw-Hill, New-York (1971)

[3] Frêne, J., Nicolas, D., Degueurce, B., Berthe, D. and Godet, M., "Lubrification hydrodynamique - Paliers et Butées", Ed. Eyrolles (1998)

[4] Özgüven, H. and Houser, D.R., "Mathematical models used in gear dynamics. A review", *Journal of Sound and Vibration*, 121, 383-411 (1988)

[5] Velex, P., "Modélisation du comportement dynamique des transmissions par engrenages", *Chapter 2 of Comportement dynamique et acoustique des transmissions par engrenagesf*, CETIM Ed., 39-95 (1993)

[6] Blankenship, G.W. and Singh, R., 1992, "A comparative study of selected mesh force interface dynamic models", *Proc. 6th ASME Power Transmission and Gearing International Conference*, Phoenix, 137-146.

[7] Kahraman, A. and Singh, R., "Non linear dynamics of a spur gear pair", Journal of sound and vibration, 142(1), 49-75 (1990)

[8] Velex, P. and Mataar, M., "A mathematical model for analyzing the influence of shape deviations and mounting errors on gear dynamic", Journal of Sound and Vibration, 191(5), 629-660 (1996)

[9] Ajmi, M. and Velex, P., "A model for simulating the quasi-static and dynamic behaviour of solid wide-faced spur and helical gears", *Mechanism and Machine Theory*, 40, 173-190 (2005)

[10] Baud, S., Velex, P., 2002, "Static and dynamic tooth loading in spur and helical geared systems. Experiments and code validation", ASME, *Journal of Mechanical Design*, 124, 334-346 (2002)

[11] Theodossiades, S. and Natsiavas, S., "On geared rotordynamic systems with oil journal bearing", *Journal of Sound and Vibration*, 243(4), 721-745 (2001)

[12] Seybert, A.F., Wu, T.W. and Wu, X.F., "Experimental validation of finite element and boundary element methods for predicting structural vibration and radiated noise", *National Aeronautics and Space Administration (NASA) Report* 19950123 083 (1994)

[13] Weber, C., Banaschek, K., "The deformation of loaded gears and the effect on their load-carrying capacity. Part 5", London: Department of Scientific and Industrial Research (Sponsored Research (Germany)) ,Report N°6 (1950)

[14] Lundberg, G., "Elastoche berürhung zweier halbraüme (Elastic contact of two half spaced)", Forschung auf dem Gebiete des Ingenieurwesens, 10 (5), 201-211 (1939)